ELSEVIER

Physica A 274 (1999) 158–170

PHYSICA A

www.elsevier.com/locate/physa

Computational test of kinetic theory of granular media

M.D. Shattuck[a], C. Bizon[b], J.B. Swift[a], Harry L. Swinney[a,*]

[a] *Center for Nonlinear Dynamics and Department of Physics, The University of Texas at Austin, Austin, TX 78712, USA*

[b] *Colorado Research Associates, 3380 Mitchell Lane, Boulder, CO 80301 USA*

Abstract

Kinetic theory of granular media based on inelastic hard sphere interactions predicts continuum equations of motion similar to Navier–Stokes equations for fluids. We test these predictions using event-driven molecular dynamics simulations of uniformly excited inelastic hard spheres confined to move in a plane. The event-driven simulations have been previously shown to quantitatively reproduce the complex patterns that develop in shallow layers of vertically oscillated granular media. The test system consists of a periodic two-dimensional box filled with inelastic hard disks uniformly forced by small random accelerations in the absence of gravity. We describe the inelasticity of the particles by a velocity-dependent coefficient of restitution. Granular kinetic theory assumes that the velocities at collision are uncorrelated and close to a Maxwell–Boltzmann distribution. Our two-dimensional simulations verify that the velocity distribution is close to a Maxwell–Boltzmann distribution over 3 orders of magnitude in velocity, but we find that velocity correlations, of up to 40% of the temperature, exist between the velocity components parallel to the relative collision velocity. Despite the velocity correlations we find that the calculated transport coefficients compare well with kinetic theory predictions.

1. Introduction

Transport and processing of granular materials is important in industries ranging from food preparation to pharmaceuticals to coal processing. However, theoretical understanding of granular flows has lagged significantly behind that of liquid and gas flows. No basic theory of granular flows comparable to the Navier–Stokes equations for fluids has attained widespread acceptance [1], and it has been argued that such a theory is not possible [2]. This lack of understanding leads to significant waste in

* Corresponding author. Fax: +1-512 471 1558.

E-mail address: swinney@chaos.ph.utexas.edu (H.L. Swinney)

0378-4371/99/$ - see front matter
PII: S0378-4371(99)00433-1

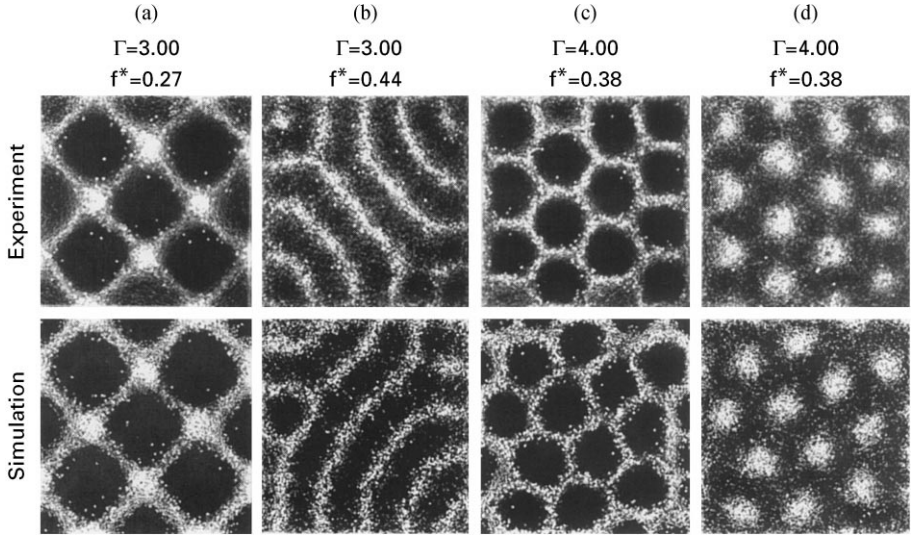

Fig. 1. Comparison of standing wave patterns obtained in experiment and an event-driven molecular dynamics simulation: (a) squares, (b) stripes, (c) and (d) alternating phases of hexagons [4]. All patterns oscillate at $f/2$. The layer depth is 5.42 times the particle diameter σ. The experiments use lead spheres sieved between 0.5 and 0.6 mm in a container which is 100σ on each side.

solids processing [3]. An increased understanding of granular flows could improve this situation.

Recent experiments [5–7] show that the patterns formed in vertically oscillated granular layers are strikingly similar to patterns seen in fluid systems (see Fig. 1).This similarity suggests that in this and other rapidly flowing granular systems, equations of motion similar to Navier–Stokes may apply. Such equations have been derived from kinetic theory for granular media flows under the assumption of binary hard sphere interactions in the limit of small energy loss in collisions [8–14]. In particular, for granular flows Jenkins and Richman [8,9] derived mass, momentum, and energy conservation equations:

$$\frac{\partial n}{\partial t} + \nabla \cdot (n\mathbf{v}) = 0\,, \tag{1}$$

$$n\frac{\partial \mathbf{v}}{\partial t} + n\mathbf{v} \cdot \nabla \mathbf{v} = -\nabla \cdot \underline{\mathbf{P}}\,, \tag{2}$$

$$n\frac{\partial T}{\partial t} + n\mathbf{v} \cdot \nabla T = -\nabla \cdot \mathbf{q} - \underline{\mathbf{P}} : \underline{\mathbf{E}} - \gamma\,, \tag{3}$$

where n is the number density, $\mathbf{v}$ is the vector velocity with components v_i, T the granular temperature (which is not the thermodynamic temperature but by analogy to molecular gases is the variance of the velocity distribution), and $E_{ij} = \frac{1}{2}(\partial_i v_j + \partial_j v_i)$ are the elements of the symmetrized velocity gradient tensor $\underline{\mathbf{E}}$. The constitutive relation

for the pressure tensor $\underline{\mathbf{P}}$ is Newton's stress law,

$$\underline{\mathbf{P}} = (P - 2\lambda \mathrm{Tr}\underline{\mathbf{E}})\mathbf{I} - 2\mu(\underline{\mathbf{E}} - (\mathrm{Tr}\underline{\mathbf{E}})\mathbf{I}) , \tag{4}$$

where Tr denotes trace and $\mathbf{I}$ is the unit tensor. For the heat flux $\mathbf{q}$, the constitutive relation is Fourier's heat law,

$$\mathbf{q} = -\kappa \nabla T . \tag{5}$$

For a two-dimensional system the equations close [9] with the equation of state, which is the ideal gas equation of state with a term that includes dense gas and inelastic effects,

$$P = (4/\pi\sigma^2)\nu T[1 + (1 + e)G(\nu)] , \tag{6}$$

and the predicted values for the transport coefficients. These are the temperature loss rate per unit volume γ, the bulk viscosity λ, the shear viscosity μ, and the thermal conductivity κ,

$$\gamma_0 = \frac{16\nu G(\nu)}{\sigma^3}(1 - e^2)\left(\frac{T}{\pi}\right)^{3/2} , \tag{7}$$

$$\lambda_0 = \frac{8\nu G(\nu)}{\pi\sigma}\sqrt{\frac{T}{\pi}} , \tag{8}$$

$$\mu_0 = \frac{\nu}{2\sigma}\left[\frac{1}{G(\nu)} + 2 + \left(1 + \frac{8}{\pi}\right) G(\nu)\right]\sqrt{\frac{T}{\pi}} , \tag{9}$$

$$\kappa_0 = \frac{2\nu}{\sigma}\left[\frac{1}{G(\nu)} + 3 + \left(\frac{9}{4} + \frac{4}{\pi}\right) G(\nu)\right]\sqrt{\frac{T}{\pi}} , \tag{10}$$

where the subscript 0 denotes predicted values, σ is the hard disk diameter and $\nu = n\pi\sigma^2/4$ is the area fraction. $G(\nu)$ is a correction for positional correlations, which are important as the density increases. $G(\nu)$ is determined from $g(r, \nu)$, the radial distribution function, which is the probability of having a pair of particles whose relative distance is in the interval $r, r + dr$ at a density ν, normalized by the same probability for an ideal gas at the same density and evaluated at $r = \sigma : G(\nu) \equiv \nu g(\sigma, \nu)$. $g(r, \sigma)$ gives the increased probability of collisions due to excluded volume in dense gases. For elastic hard disks, $G(\nu)$ is often described by a formula derived by Carnahan and Starling [15],

$$G_{CS}(\nu) = \frac{\nu(16 - 7\nu)}{16(1 - \nu)^2} . \tag{11}$$

Eq. (11) works well for elastic particles if the solid fraction is below 0.675, where a phase transition occurs [16], and is often used in modeling granular media [9]. $G(\nu) \equiv \nu g(\sigma, \nu)$ defines G in terms of the radial distribution function $g(r, \nu)$, evaluated at $r = \sigma$, while (11) is a particular model for G, denoted by the subscript CS.

The equations of motion (1)–(3) differ slightly from the dense gas Navier–Stokes equations by the addition of a temperature loss rate term (7) in the energy equation (3)

and in the equation of state for the pressure (6), which depends on the ratio of the normal relative velocity v_n of a colliding pair after a collision to v_n before a collision (i.e., the coefficient of restitution e). Eq. (7) was derived for a coefficient of restitution which is independent of v_n, but in real materials e is a function of v_n [17]. In our simulation, we allow e to vary as [4]

$$e(v_n) = \begin{cases} 1 - Bv_n^{\beta}, & v_n < v_a, \\ \varepsilon, & v_n > v_a, \end{cases} \tag{12}$$

where v_n is the component of relative velocity along the line joining particle centers (normal to the contact surface), $B = (1-\varepsilon)(v_a)^{-\beta}$, $\beta = \frac{3}{4}$, ε is a constant, chosen to be 0.7, and v_a is effectively set to unity as it is the velocity scale used to nondimensionalize all quantities to follow. By use of (12) a new volumetric loss rate γ_e is determined [18].

$$\gamma_e = \frac{4\nu G\sqrt{T}}{\sigma^3\pi^{3/2}} \left[(1-e_0^2)(v_a^2+4T)\exp(-v_a^2/4T) + 4I\right] , \tag{13}$$

where

$$I = 2^{1+\beta}AT^{1+\beta/2}(\Gamma(2+\tfrac{1}{2}\beta) - \Gamma(2+\tfrac{1}{2}\beta, v_a^2/4T)) \\ -A^2 2^{2\beta}T^{1+\beta}(\Gamma(2+\beta) - \Gamma(2+\beta, v_a^2/4T)) , \tag{14}$$

$\Gamma(a)$ is the gamma function, and $\Gamma(a,b)$ is the incomplete gamma function. In the limit that $v_a \to 0$, $\gamma_e \to \gamma_0$.

A further assumption used in deriving (7) for γ is molecular chaos (i.e., no velocity–velocity correlations). Molecular chaos assumes that the velocity–velocity distribution function $\Theta_2(\mathbf{v}_1, \mathbf{v}_2)$ equals the product of the single-particle velocity distribution of particle 1, $\Theta(\mathbf{v}_1)$, and the single-particle velocity distribution of particle 2, $\Theta(\mathbf{v}_2)$. However, γ can be determined without regard to the form of $\Theta_2(\mathbf{v}_1, \mathbf{v}_2)$ as

$$\gamma = \frac{(1-e^2)G}{\sigma} \frac{\langle v_n^2 \rangle_c}{\langle v_n \rangle_c} nT , \tag{15}$$

where e is the constant coefficient of restitution, and

$$\langle h(\mathbf{v}_1, \mathbf{v}_2) \rangle_c = \int_{\text{all collisions}} h(\mathbf{v}_1, \mathbf{v}_2)\Theta_2(\mathbf{v}_1, \mathbf{v}_2)\, d\mathbf{v}_1\, d\mathbf{v}_2 . \tag{16}$$

$h(\mathbf{v}_1, \mathbf{v}_2)$ is any function of the collision velocities. If the distribution of relative normal velocity at collision is equal to that predicted by molecular chaos, $P(v_n) = (1/2T)v_n \exp(-v_n^2/4T)$, then $\langle v_n^2 \rangle_c = 4T$ and $\langle v_n \rangle_c = \sqrt{\pi T}$, so that $\gamma = \gamma_0$ is recovered.

While (1)–(10) have been available for 15 years, there have been few experimental [19–21] or numerical [18,22–24] tests. In this paper we will directly test the validity of these equations, using event-driven molecular dynamics simulations. Experiments such as those in vibrated layers of granular materials provide an unprecedented opportunity to study granular fluid-like behavior. However, experiments alone do not provide information on the microscopic underpinnings of the kinetic theory description, due to

the difficulty of internal measurements in three-dimensional systems. To overcome this difficulty we have developed an event-driven molecular dynamics simulation capable of quantitatively reproducing laboratory experiments [4] in vertically oscillated granular media, including wavelength-changing secondary instabilities [25]. The simulation is based on assumptions similar to those for granular kinetic theory. In particular, particles obey Newton's laws between binary instantaneous collisions (hard sphere model) that conserve momentum but dissipate energy. However, unlike the kinetic theory models, the energy dissipation can be large, and there is no restriction on the velocity distribution.

In Section 2 we describe the simulation technique and discuss its quantitative verification with experiments in vertically oscillated shallow granular media. In Section 3 we describe tests of the assumptions and results of kinetic theory.

2. Numerical model

The purpose of simulations of our model is to test granular kinetic theory assumptions and predictions. However, to determine if granular kinetic theory applies to real granular materials we must first validate our simulation by comparison with experiments. For this purpose we have chosen a vertically oscillated thin granular layer that shows the kind of fluid-like behavior to which kinetic theory is likely to apply. In this system a thin layer of granules is vertically oscillated by an electromagnetic shaker. Different patterns emerge for various shaking amplitudes and frequencies [5–7] (see Fig. 1).

2.1. Vertically oscillated granular layer

We have developed an event-driven numerical simulation of hard spheres interacting through momentum conserving, energy dissipating collisions [4]. In this type of simulation [26,27] time advances from collision to collision with ballistic motion between collisions. A sorted list of the time-to-next-collision for each particle is used to determine when the next collision will occur. The simulation performs the collision using an operator which maps the velocities of each particle before the collision to their values after the collision. Collisions conserve momentum but not energy. The collision duration is assumed zero, therefore limiting the particle interactions to binary collisions. Energy is lost in collisions through a normal coefficient of restitution e defined by the ratio of the outgoing normal relative velocity v_n to the incoming v_n. Therefore, energy is lost at a rate of $1-e^2$ per collision. e is a function of v_n given by (12), which is consistent with real materials [28] and prevents the numerical instability of inelastic collapse [17].

To validate the simulation, we conducted experiments in a vertically oscillated cell $100\sigma \times 100\sigma$ with $60\,000 \pm 8$ lead spheres ($\sigma = 0.55$ mm) [4]. Experiments and simulations under the same conditions are compared in Fig. 1 using the nondimensional frequency $f^* = f\sqrt{H/g}$, where f is the frequency of oscillation, H is the height of the

layer, and g is the acceleration of gravity and the nondimensional maximum oscillation acceleration amplitude is $\Gamma = A(2\pi f)^2/g$, where A is the maximum stroke amplitude.

Three collisional particle properties — the coefficient of friction μ, the value of the constant portion of normal coefficient of restitution ε (see (12)), and the cutoff for the rotation coefficient of restitution β_0 — must be determined for the simulation. For the comparison to experiments, β_0 is taken from the literature [29], and ε and μ are determined by adjusting their values until the pattern wavelength in the simulation and experiment matched in two specific runs. For the comparisons to the kinetic theory, rotation is ignored and therefore β_0 and μ are not needed. This is consistent with the kinetic theory, which also ignores rotation.

The results of the simulation for various control parameters are shown in Fig. 1. Patterns obtained in the simulation and experiment at the same values of the control parameters show a striking correspondence. Further, the pattern wavelengths for various f^* in experiment and simulation agree well, even when comparing the simulation in a cell 100σ wide with experiments in a large container with a diameter of 982σ.

2.2. Randomly accelerated forcing of particles in a box with no gravity

For comparison to kinetic theory we restrict our full three-dimensional simulation (which includes particle rotations) to two dimensions and to particles that do not rotate. We use a periodic cell which is 52.6σ on each side; the number of particles determines the density of the granular gas. The particles interact through the velocity-dependent coefficient of restitution described by (12). In elastic hard sphere models, transport properties, velocity distributions, velocity correlations, and $G(v)$ can all be determined from simulations at thermal equilibrium. For inelastic hard sphere models, because of the energy loss, the equilibrium state is for all particles to be at rest. Therefore, we constantly add energy in a stochastic manner (random accelerated forcing) to achieve a steady state at finite temperature. The situation is opposite that in simulations on non-equilibrium systems of elastic particles, where the constant energy input from the driving must be removed through an artificial means [30].

In our model each particle moves under a uniform acceleration:

$$\mathbf{a}_i = a_0\hat{\mathbf{r}}_i \,. \tag{17}$$

The magnitudes of all particle accelerations, a_0, are the same, but the directions, $\hat{\mathbf{r}}_i$, are randomly and uniformly chosen. When a collision occurs, two particles are given new $\hat{\mathbf{r}}_i$. In order to conserve total momentum, we hold the total acceleration of the particles at zero by giving exactly opposite accelerations to pairs of particles. Initially, each particle is paired with another, and these are given opposite accelerations. Later, when one particle is chosen and its acceleration randomized, its partner particle is also given a new acceleration, opposite to the first particle's. The random acceleration model is chosen because it closely models thin flat disks on an air table [18,31]. This correspondence with an experimentally realizable system can be exploited in the future

to directly test kinetic theory against a physical system. This type of forcing has several technical implications for the simulation which are described in Ref. [18].

Spatially uniform application of the accelerated forcing model to an inelastic gas of hard disks produces a homogeneous steady state. From this state we extract the velocity distribution function, velocity–velocity correlations, $G(v)$, and the temperature loss rate γ for various constant densities and temperatures. To extract the shear viscosity and the thermal conductivity we introduce a spatially dependent heating to produce either a velocity gradient to measure viscosity or a temperature gradient to measure thermal conductivity.

3. Tests of granular kinetic theory

In this section we test granular kinetic theory against our validated event-driven molecular dynamics simulation of a two-dimensional granular gas heated by random acceleration. Comparison of other types of heating as well as more detailed analysis of our results can be found in Ref. [18].

3.1. Test of assumptions

3.1.1. Velocity distribution functions

To obtain (1)–(10) it is assumed that the deviations of the velocity distribution $\Theta(v)$ of an inelastic hard sphere gas from a Maxwell–Boltzmann distribution can be expanded in a polynomial in the velocity. The lowest-order term of the expansion is unity, corresponding to a $\Theta(v)$ equal to the Maxwell–Boltzmann distribution, which is the distribution for an unheated elastic gas. To test this assumption for the steady-state that is produced by accelerated forcing, we determine the velocity distribution for various temperatures and densities and find that $\Theta(v)$ is close to the Maxwell–Boltzmann distribution, as seen in Fig. 2. The deviations which do exist become stronger as the density and temperature increase. Because of the velocity-dependent coefficient of restitution (12), increasing temperature has the same effect as decreasing the average coefficient of restitution due to lower average collision velocities. These deviations tend to flatten the distribution, increasing the probability in the tails and slightly in the peak, and decreasing the probability in between [18]. Similar types of deviations, but much stronger, have been observed in experiments on a dilute, vertically oscillated granular layer [21].

3.1.2. Velocity–velocity correlations

A further assumption of kinetic theory is that of molecular chaos — that the particle velocities involved in a collision are uncorrelated. Strong velocity correlations have been reported in driven granular media [32–34], and so we measure velocity–velocity correlation functions to test the kinetic theory assumption. Given two particles, labeled 1 and 2, $\hat{\mathbf{k}}$ is a unit vector pointing from the center of 1 to the center of 2. Particle 1's

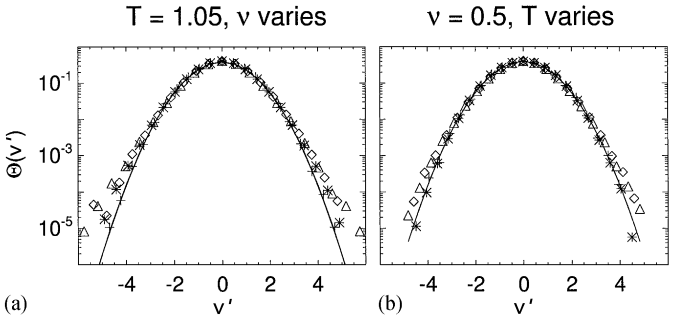

Fig. 2. Velocity distribution function $\Theta(v')$ for accelerated forcing, compared to Maxwell–Boltzman distributions (solid curves). The velocities are scaled with the square root of the temperature T, so that $v' = v/\sqrt{T}$ and $\Theta(v') = P(v')\sqrt{T}$, where $P(v')$ is the probability distribution of v'. In (a) the average temperature is approximately 1.05, and the solid fraction is varied (+: $\nu = 0.1$, $*$: $\nu = 0.4$, $\diamondsuit$: $\nu = 0.6$, $\triangle$: $\nu = 0.8$). In (b) ν is fixed at 0.5 and the temperature is varied (+: $T = 3.0 \times 10^{-5}$, $*$: $T = 1.1 \times 10^{-2}$, $\diamondsuit$: $T = 1.05$, $\triangle$: $T = 256$).

velocity then has a component $v_1^{\parallel}$ parallel to and $v_1^{\perp}$ perpendicular to $\hat{\mathbf{k}}$; likewise for particle 2. We define two correlation functions

$$\langle v_1^{\parallel} v_2^{\parallel} \rangle = \sum v_1^{\parallel} v_2^{\parallel} / N_r \,, \tag{18}$$

$$\langle v_1^{\perp} v_2^{\perp} \rangle = \sum v_1^{\perp} v_2^{\perp} / N_r \,, \tag{19}$$

where the sums are over N_r particles such that the distance between the two particles is within δr of r. If particle velocities are uncorrelated, $\langle v_1^{\parallel} v_2^{\parallel} \rangle$ and $\langle v_1^{\perp} v_1^{\perp} \rangle$ will both give zero.

The parallel and perpendicular velocity correlations are plotted in Fig. 3 for particles driven with randomly accelerated forcing. Strong long-range velocity correlations are apparent. These correlations are not small, reaching as much as 40% of the temperature; typically, the perpendicular correlations are about one-half of the parallel correlations. Further, these correlations are long range — they extend the full length of the system. The parallel correlations drop to zero at $L/2$, while the perpendicular correlations reach zero around $r = 10\sigma$, and have a negative value but zero derivative at $L/2$. The long-range nature of the correlation is not due to the size of the computational cell. Similar cell-filling correlations were observed in cells 4, 16, and 64 times larger in area [24].

3.1.3. Equation of state

The virial theorem of mechanics as applied to hard spheres can be used to calculate the equation of state [35,36],

$$PV = NT + \frac{\sigma}{2t_m} \sum_c \hat{\mathbf{k}} \cdot \Delta \mathbf{v}_i \,, \tag{20}$$

where N is the total number of particles, V is the total volume, and the sum is over all collisions that occur during the measurement time t_m, $\Delta \mathbf{v}_i$ is the change in the

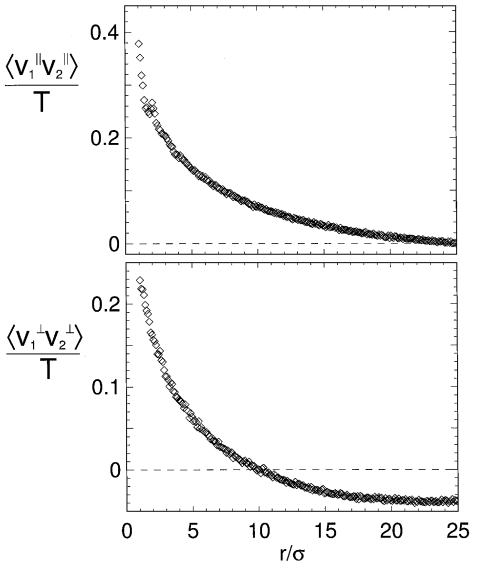

Fig. 3. Velocity correlations as a function of particle separation at $v = 0.5$, $T = 1.05$ for accelerated forcing in a box of length 52.6σ. The curve is constructed from 100 frames separated in time by 100 collisions per particle, and $\delta r = \sigma/10$.

velocity of the ith particle due to the collision, and $\hat{\mathbf{k}}$ is the unit vector pointing from particle center to particle center. In this form, measurement of pressure reduces to measurement of the average particle energy and the average change in the normal velocity at collision.

Using (20) to measure pressure, and assuming the equation of state (6), we produce a measurement of $G(v)$, denoted $G_s(v)$, where the subscript s stands for simulation. This measured value of G is compared to the Carnahan and Starling value $G_{CS}(v)$ from (11) and is shown in Fig. 4. Accurate characterization of $G(v)$ is important, because it occurs in the expressions for transport coefficients. $G_{CS}(v)$ consistently overestimates $G_s(v)$ above $v = 0.25$ with increasing error until $v > 0.675$, where elastic particles undergo a phase transition to an ordered state [16], and the two curves begin to converge and finally cross at $v = 0.8$.

3.2. Test of transport coefficient predictions

3.2.1. Volumetric temperature loss rate

We calculate the volumetric temperature loss rate γ for the simulation and compare to the kinetic theory value including the correction for the velocity-dependent coefficient of restitution γ_e (13), as shown in Fig. 5. The agreement is quite good but there is a systematic overestimate as T or v is increased. This deviation can be explained by velocity correlations discussed above. Velocity correlations change the values of $\langle v_n^2 \rangle_c$ and $\langle v_n \rangle_c$, which determine γ through (15). The ratio $\langle v_n^2 \rangle_c$ to $\langle v_n \rangle_c$, normalized by

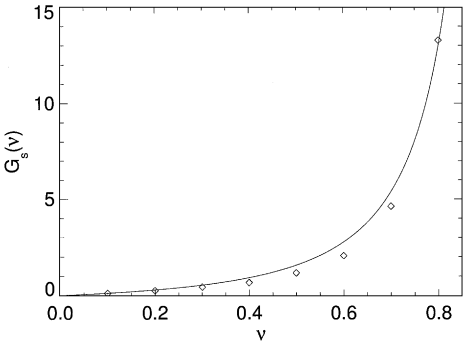

Fig. 4. (a) $G_s(\nu)$ for inelastic hard discs driven by accelerated forcing for $T = 1.05$ (open symbols). The solid curve is the Carnahan and Starling relation $G_{CS}(\nu)$, given by (11).

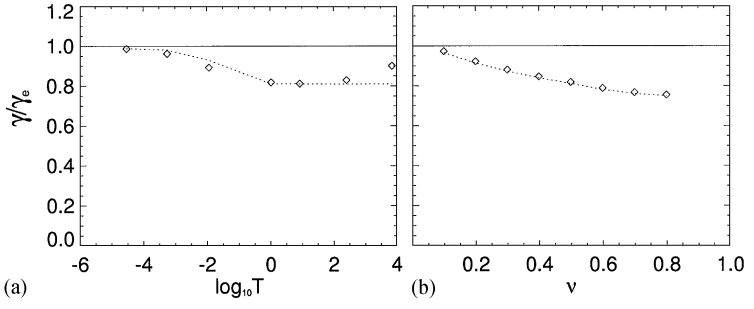

Fig. 5. Ratio of the temperature loss rate γ from molecular dynamic simulations to the prediction of kinetic theory (13) γ_e as a function of (a) temperature with $\nu = 0.5$ and (b) density with $T = 1.05$. The dotted lines show $(\sqrt{\pi}/4\sqrt{T})\langle v_n^2\rangle_c/\langle v_n\rangle_c$ (see (15)).

the molecular chaos value $4\sqrt{T/\pi}$ tracks the values obtained in the simulation closely; see Fig. 5.

3.2.2. Thermal conductivity and shear viscosity

In order to measure the thermal conductivity and shear viscosity of the heated inelastic gas we introduce spatially dependent heating. Spatial inhomogeneity in the magnitude of the forcing leads to a stationary inhomogeneous temperature field, allowing measurement of heat flux and thermal conductivity κ; spatial inhomogeneity in the mean of one forcing component leads to a stationary inhomogeneous velocity field, allowing measurement of the momentum flux and the shear viscosity μ. The results of these calculations are shown in Fig. 6. While κ agrees well at low temperatures, there is a sizable error of 50% compared to the value predicted by the kinetic theory proposed by Jenkins and Richman [9]. One problem with this result is that in order to extract κ, Fourier's Law (5) must be assumed, providing no independent test of this relation. Analysis based on other closures of the Boltzmann equation predict a term in the heat flux proportional to the density gradient [37]. If such a term had a sizeable magnitude and were ignored, it would cause a reduction in the observed κ.

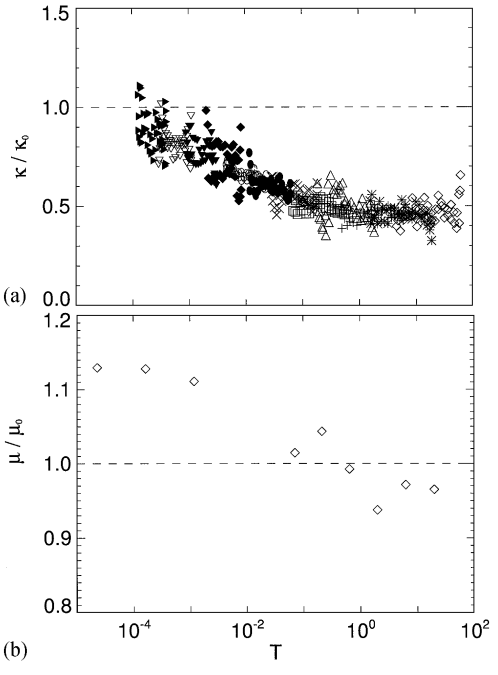

Fig. 6. (a) Ratio of the thermal conductivity κ measured from simulations to κ_0 from kinetic theory (10). Each symbol denotes a different run; for each run, the average solid fraction is 0.75. (b) Viscosity, normalized by the kinetic theory value μ_0, as a function of T, for $v = 0.6$.

The determination of μ, however, allows us, for each run at fixed T, to test Newton's viscosity law (4),

$$P_{yz} = -\mu \frac{\partial v_y}{\partial z} , \tag{21}$$

where the viscosity μ is a constant of proportionality. We find that the linear relation of (21) holds and the slope of these curves then provide values for μ which are compared to the kinetic theory result from (9) and shown in Fig. 6(b). The maximum deviation is less than 15%. Unlike the loss rate and thermal conductivity, the shear viscosity is underestimated by kinetic theory at lower temperatures. However, the trend of decreasing transport with increasing T is the same.

4. Conclusions

We find that granular kinetic theory assumptions and predictions agree well with event-driven molecular dynamics simulations of a two-dimensional inelastic granular gas. Our simulation has been validated quantitatively with laboratory experiments of vertically oscillated thin granular layers. Further, the simulation has shown that the local velocity distribution in a vibrated layer is close to a Maxwell–Boltzmann

distribution [38]. This suggests that the kinetic theory should apply to that system as well. In particular, kinetic theory assumes that velocities are distributed according to a Maxwell–Boltzmann distribution, and that at collisions there is no velocity correlation. Both of these are determined directly in our simulations. We find a Maxwell–Boltzmann distribution over 3 orders of magnitude in velocity (Fig. 2), but we find that velocity correlations of up to 40% exist between the velocity components parallel to the relative collision velocity (Fig. 3). Kinetic theory also predicts the form of the closure relations and the values of the transport coefficients in those relations. We determined the volumetric loss rate coefficient, which agrees with theory within 20% (Fig. 5); the origin of this difference is the substantial velocity correlation mentioned above. We find that the shear stress depends linearly on the shear velocity gradients, yielding the predicted Newtonian stress law with a shear viscosity that deviates less than 15% in the worst case from the value determined by kinetic theory (Fig. 6(b)). Using our current technique we cannot determine if Fourier's cooling law is obeyed, but under the assumption that it is, a thermal conductivity can be calculated; it has a maximum deviation from theory of 50% (Fig. 6(a)). We have also found that the value of the radial distribution function evaluated at the particle diameter, which is used to correct for spatial correlations that develop as the density is increased, is systematically overestimated by the value predicted by Carnahan and Starling above a volume fraction ν of about 0.25 (Fig. 4). Even for elastic particles, kinetic theory is not expected to work to arbitrarily high solid fractions; as density increases, deviations from kinetic theory are expected. Further as the inelasticity of particles increases, velocity correlations increase, reducing collisional transport. However, despite these difficulties the theory agrees remarkably well with the results of simulations.

Acknowledgements

This work was supported by the Engineering Research Program of the Office of Basic Energy Sciences of the US Department of Energy, and NSF — International Program (Chile).

References

[1] H.M. Jaeger, S.R. Nagel, R.P. Behringer, Phys. Today 49 (1996) 32.
[2] L.P. Kadanoff, Rev. Mod. Phys. 71 (1999) 435.
[3] E.W. Merrow, Chem. Eng. Progr. 81 (1985) 14.
[4] C. Bizon, M.D. Shattuck, J.B. Swift, W.D. McCormick, H.L. Swinney, Phys. Rev. Lett. 80 (1998) 57.
[5] F. Melo, P. Umbanhowar, H.L. Swinney, Phys. Rev. Lett. 72 (1994) 172.
[6] F. Melo, P.B. Umbanhowar, H.L. Swinney, Phys. Rev. Lett. 75 (1995) 3838.
[7] P. Umbanhowar, F. Melo, H.L. Swinney, Nature 382 (1996) 793.
[8] J.T. Jenkins, M.W. Richman, Arch. Rat. Mech. Anal. 87 (1985) 355.
[9] J.T. Jenkins, M.W. Richman, Phys. Fluids 28 (1985) 3485.
[10] J.T. Jenkins, M. Shahinpoor, in: J.T. Jenkins, M. Satake (Eds.), Mechanics of Granular Materials: New Models and Constitutive Relations, Elsevier, Amsterdam, 1983, p. 339.

[11] C.K.K. Lun, S.B. Savage, D.J. Jeffrey, N. Chepurniy, J. Fluid Mech. 140 (1983) 223.
[12] C.K.K. Lun, S.B. Savage, Acta Mech. 63 (1986) 15.
[13] C.K.K. Lun, J. Fluid Mech. 233 (1991) 539.
[14] A. Goldshtein, M. Shapiro, J. Fluid Mech. 282 (1995) 75.
[15] N. F. Carnahan, K.E. Starling, J. Chem. Phys. 51 (1969) 635.
[16] B.J. Alder, T.E. Wainwright, Phys. Rev. 127 (1962) 359.
[17] D. Goldman, M.D. Shattuck, C. Bizon, W.D. McCormick, J.B. Swift, H.L. Swinney, Phys. Rev. E 57 (1998) 4831.
[18] C. Bizon, M.D. Shattuck, J.B. Swift, H.L. Swinney, Phys. Rev. E (1999), in press.
[19] T.G. Drake, J. Fluid Mech. 225 (1991) 121.
[20] J. Delour, A. Kudrolli, J.P. Gollub, preprint, 1998.
[21] J.S. Olafsen, J.S. Urbach, Phys. Rev. Lett. 81 (1998) 4369.
[22] C.S. Campbell, Annu. Rev. Fluid Mech. 2 (1990) 57.
[23] E.L. Grossman, T. Zhou, E. Ben-Naim, Phys. Rev. E 55 (1997) 4200.
[24] C. Bizon, M.D. Shattuck, J.B. Swift, H.L. Swinney, in: J. Karkheck (Ed.), Dynamics: Models and Kinetic Methods for Nonequilibrium Many-Body Systems, NATO ASI Series E: Applied Sciences, Kluwer Academic publishers, Dordrecht, 1999, in press.
[25] J.R. de Bruyn, C. Bizon, M.D. Shattuck, D. Goldman, J.B. Swift, H.L. Swinney, Phys. Rev. Lett. 81 (1998) 1421.
[26] M. Marín, D. Risso, P. Cordero, J. Comput. Phys. 109 (1993) 306.
[27] B.D. Lubachevsky, J. Comput. Phys. 94 (1991) 255.
[28] W. Goldsmith, Impact, Edward Arnold Ltd., London, 1960.
[29] O.R. Walton, in: M.C. Roco (Ed.), Particulate Two-Phase Flow, Butterworth-Heinemann, Boston, 1993, pp. 884–911.
[30] D.J. Evans, G.P. Morriss, Statistical Mechanics of Nonequilibrium Liquids, Academic Press, San Diego, 1990.
[31] L. Oger, C. Annic, D. Bideau, R. Dai, S.B. Savage, J. Stat. Phys. 82 (1996) 1047.
[32] M.R. Swift, M. Boamfã, S.J. Cornell, A. Maritan, Phys. Rev. Lett. 80 (1998) 4410.
[33] J.A.G. Orza, R. Brito, T.P.C. van Noije, M.H. Ernst, Int. J. Mod. Phys. C 8 (1998) 953.
[34] T.P.C. van Noije, M.H. Ernst, E. Trizac, I. Pagonabarraga, Phys. Rev. E 59 (1999) 4326.
[35] J.O. Hirschfelder, C.F. Curtiss, R.B. Byrd, Molecular Theory of Gases and Liquids, Wiley, New York, 1954.
[36] D.C. Rapaport, The Art of Molecular Dynamics Simulation, Cambridge University Press, Cambridge, 1980.
[37] J.J. Brey, J.W. Duffy, A. Santos, J. Stat. Phys. 87 (1997) 1051.
[38] C. Bizon, Ph.D. Thesis, University of Texas, Austin, 1998.